

CONTROL SYSTEM DEVELOPMENTS AND MACHINE MODEL BENCHMARK FOR THE GSI FRAGMENT SEPARATOR FRS*

J. P. Hucka[†], J. Enders, Technische Universität Darmstadt, Darmstadt, Germany
S. Pietri, H. Weick, D. Ondreka, J. Fitzek, B.R. Schlei
GSI Helmholtzzentrum für Schwerionenforschung, Darmstadt, Germany

Abstract

At the GSI Helmholtzzentrum für Schwerionenforschung and at the future FAIR facility the LHC Software Architecture LSA will be used for a new control system for accelerators, beam transfers and storage rings. In addition, the fragment separator FRS and - at a later stage - also the superconducting fragment separator Super-FRS at FAIR will be controlled within this framework. In fragment separators of in-flight facilities, the interaction of the beam with matter in the beamline and the beam's associated energy loss needs to be taken into account. This energy loss is calculated using input from ATIMA and has been included into the code of the LSA framework. The setting generator was simulated and benchmarked by comparison to results of earlier measurements. The modeling of slits and their magnetic-rigidity-changing properties as well as modeling of the propagation of charge states and isotopes through matter was included.

FRS

The FRS is a high resolution magnetic forward spectrometer with a maximum magnetic rigidity of 18 Tm and a momentum and angular acceptance of ± 1 and ± 7.5 mrad, respectively [1]. It is used to separate and identify reaction products from nuclear reactions such as fission or fragmentation of heavy-ion beams with matter. It consists of 9 focal planes with 1 dipole (green) and 5 quadrupole (yellow) magnets in between each plane to allow separation and beam focussing (Fig. 1). Furthermore the FRS is equipped with multiple multi-wire-proportional chambers (MWPC), time-projection-chambers (TPC), scintillators (SCI), ionization chambers (IC), targets, and degraders to allow mass and charge of the ions to be identified in flight on an event-by-event basis.

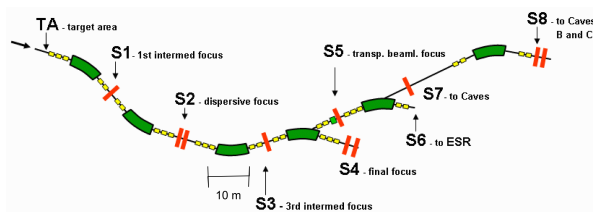


Figure 1: Magnetic setup of FRS and focal planes. [2]

In 1990 the FRS has been completed at the GSI Helmholtzzentrum für Schwerionenforschung and has been

* Work supported by BMBF (05P15RDFN1 and 05P19RDFN1)

[†] j.-p.hucka@gsi.de

in operation ever since. With the construction of the new FAIR facility (Facility for Antiproton and Ion Research [3]), the existing GSI facility is currently being upgraded to accommodate the current experimental beam time of FAIR-Phase-0 and future beam times at both the GSI and FAIR facilities [4]. Following the completion of FAIR, the facility will feature also a new superconducting fragment separator (Super-FRS [5]) with enhanced acceptance.

CONTROL SYSTEM

Following the upgrade, the GSI/FAIR facility will provide heavy-ion beams at higher intensities than before. With the construction of the new FAIR center, a control system upgrade is also required in order to provide streamlined operability for the combined GSI/FAIR facility for increased operation efficiency. These control system upgrades encompass both hard- and software.

Hardware

Like in GSI's main control room, the hardware for the FRS controls has been replaced. Figure 2 shows the old control panels and the refurbished control room of the FRS in comparison. Old consoles and computers - operating on a VMS platform - have been removed. New computers operating on Linux and Windows 10 and monitors were installed. A set of 2x3 monitors and 2 computers is dedicated to the operation and controlling of the FRS by using a combination of the LSA [6] framework and applications additional to self developed monitoring applications for pneumatic drives and stepper motors, called DRIVESTAT, dipoles, quadrupoles and sextupoles, with FMGSTAT, and FMGSKAL, which is being used to launch the magnetic pre-cycling sequence outside of the LSA framework. DRIVESTAT and FMGSTAT communicate both with LSA and the devices directly to read out and monitor LSA setting values, set device values, current device values and status reports. Next to it monitors and a dedicated computer is placed for calculation and online simulation purposes utilizing LISE++ [7] and MIRKO [8]. On top of this set up a big monitor is used for online detector readout via ROOT [9].

The new setup facilitates access to the FRS controls via LSA, other monitoring applications, simulations tools and online detector readout. The equipment thus allows an efficient interplay between simulation, experimental data on beam properties and controls to be implemented.

Content from this work may be used under the terms of the CC BY 3.0 licence (© 2019). Any distribution of this work must maintain attribution to the author(s), title of the work, publisher, and DOI.



Figure 2: Control room update at the FRS. Left: old panels and consoles from the 90s. Right: new set up and monitors.

LSA and Machine Model

The LHC Software Architecture (LSA) is a JAVA framework and has been licensed in 2007 to GSI from CERN and has been in continuous development for the GSI and upcoming FAIR facility to provide the data supply for all devices and machines in both facilities [10]. In order to achieve this goal and the aforementioned requirements, the following three paradigms drive the control-system developments:

- decentralization by separation and distribution of devices, databases, GUIs, client applications and logics (e.g., setting generation),
- modularity by self-contained modules and APIs (application programming interface) with well defined tasks inside the LSA core,
- layering by enclosed levels of abstraction working independently from each other and communicating via APIs,

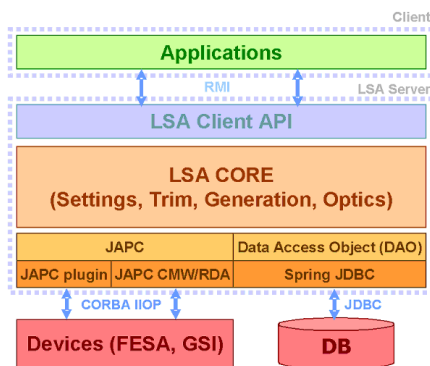


Figure 3: Layers of abstraction from application to device [11]. The APIs in use are the LSA client API, JDBC (Java Database Connectivity) and JAPC (Java API for Parameter Control) between LSA and FESA (Frontend Software Architecture)

Figures 3 and 4 show the architecture in use for realizing the development paradigms. The framework consists of three layers. The client's side hosts applications and GUIs used for controlling and monitoring devices, patterns and settings. The LSA Server layer is responsible for the communication between the clients, the LSA server, the databases and devices via dedicated APIs. Additionally the LSA Core, where setting generation, calculation, manipulation and persistence take place resides on the server. On the lowest layer are devices and different databases which are either used to provide different information for the core, e.g., calibration curves, optics or device data, or store information from the core, i.e., settings.

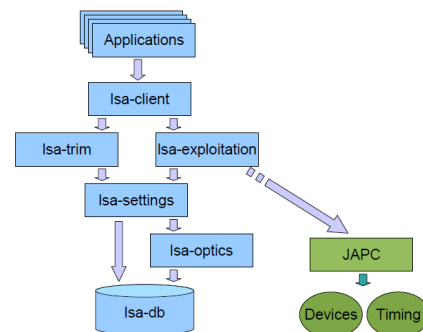


Figure 4: Workflow and modules inside LSA from top to bottom. Detailed names of the LSA core modules.

In order to utilize the capabilities of the LSA Core a so-called machine model has to be designed to generate settings and manipulate them. Different concepts are used within a model for individual machines and devices:

- Context: defines a time interval, e.g., see Pattern, in which a parameter possesses a value

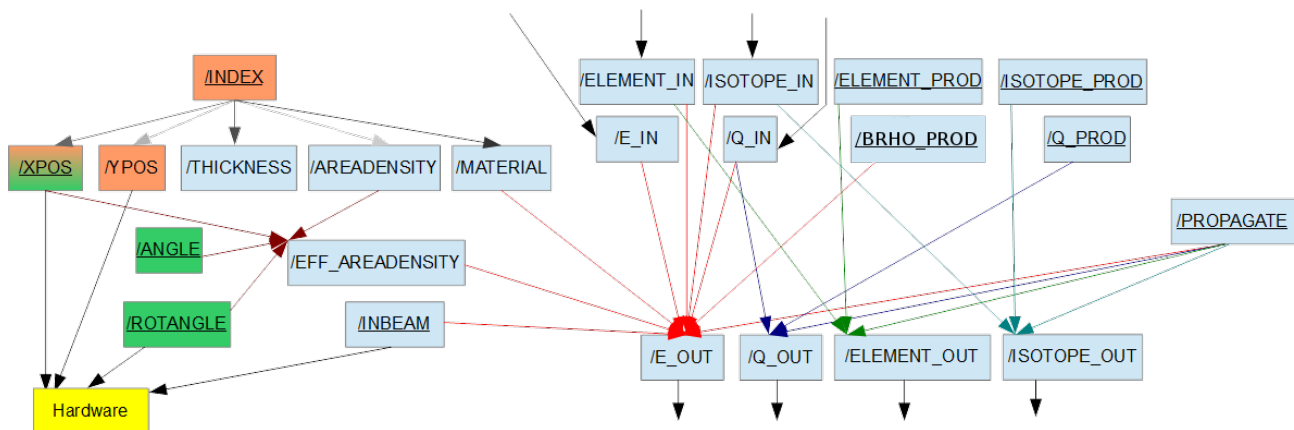


Figure 5: FRS parameter hierarchy for matter visualizing which parameters contribute to the calculation of settings for other parameters. Light blue parameters are shared by all devices, orange is additional for target ladders and green is additional for degraders. Arrows of the same colour belong to the same makerule. Underlined parameters are required input by the operator. Black arrows on top are output parameters of previous matter. Outgoing energy, charge, element number, isotope number are transferred to the respective incoming parameters of subsequent matter.

- Pattern: defines which beam production chain is active and provides timing
- Beam Production Chain: describes the path of a beam from the inception (source) to destruction (target)
- Parameter: a measurable or defined variable of a respective type within a hierarchy
- Setting: a value belonging to a parameter during a certain beamprocess
- Beamprocess: defines a specific process within a context
- Makerule: defines how settings are calculated between different parameters

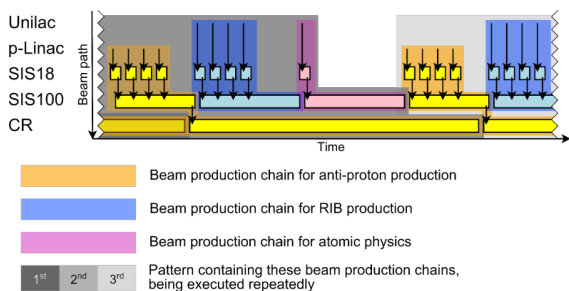


Figure 6: New pattern and beam production chain concepts visualized. While an experiment runs in the CR, the linear accelerators provide ion beams for the SIS18 and SIS100 in parallel for different experiments.

These concepts are visualized in Fig. 5 and Fig. 6, respectively, which shows the newly developed FRS machine model for setting generation and manipulation. The FRS machine model has been designed with the goal in

mind to provide online energy-loss calculations for the different types of matter used during the operation of the FRS as well as other machines. These types of matter are targets, detectors, target ladders, degrader wedges, disks and ladders. For the actual calculation a pre-calculated ATIMA 1.41 [12] spline for the proper beam and target combination is read out by the respective makerule, which uses the settings of the parameters /MATERIAL, /ELEMENT_IN, /ISOTOPE_IN, /Q_IN, /E_IN and /EFF_AREADENSITY in Fig. 5 as input. Furthermore the machine model is capable of handling the production of secondary beams inside the respective matter by specific input of the operator, which was precalculated using other respective simulation software, i.e., LISE++. From this machine model the benefit is provided that the beam changing nature of matter inside accelerators or transfer lines is being accounted for and therefore ion optical elements following said matter can be automatically set to the right magnetic rigidity of the beam and consequently the current necessary to produce the respective magnetic fields, given that the operator provides the properties of the produced secondary beam, see parameters with suffix PROD in Figure 5, making the precalculation of initial settings for a primary beam outside of LSA and the model obsolete. The accuracy of the model will be further discussed in the benchmark section.

Sequences

Ensuring further operability of the FRS does not only include matter but also ion-optical elements. FRS specific sequences regarding magnets and drives are processes with well defined steps within the Sequencer [13], which is a framework developed and maintained at the GSI to automate device-testing procedures and enable direct device manipulation, e.g., setting a current for power converters outside of the LSA framework. The developed sequences are the magnetic pre-cycling of magnets and the drive sequence,

Content from this work may be used under the terms of the CC BY 3.0 licence (© 2019). Any distribution of this work must maintain attribution to the author(s), title of the work, publisher, and DOI.

which reads out from LSA and drives the respective matter inside the FRS.

A pre-cycling sequence had to be developed in order to take the magnetic hysteresis of ion optical elements into account, which would prohibit an unambiguous relation between the current set value and the desired $B\rho$. Therefore a magnetic pre-cycling with the following steps was programmed:

- Step 1: Ramp current up to maximum value in 15 s and wait 15 s to achieve saturation.
- Step 2: Ramp current down to 0 A in 15 s and wait 15 s to achieve relaxation.
- Step 3: Repeat step 1 and 2 two more times. Ramp up to new current value.

This procedure was successfully tested within the sequencer on one magnet and on a set of magnets in parallel. It is the operators' duty to run this sequence before a relative change in $B\rho$ of more than 1 % occurs during operation. An automatic start of this sequence is not foreseen, since it would halt every machine and experiment connected via the FRS for at least 3 minutes and would not allow for parallel operation. The magnetic precycling is embedded within a dedicated application.

The drive sequence, was needed due to LSA's inability to communicate with the drives' front-end architecture. This sequence is embedded within the DRIVESTAT application and checks continuously if the position of matter inside the FRS machine model in LSA has been changed. If a change exists, this change is then propagated to the corresponding hardware drive and moved accordingly. A successful test has been conducted of the drive sequence and can therefore be used for future beam times.

BENCHMARK

Setup

Similar to [14] the new updated machine model was benchmarked with experimental magnet setting from old beam times. For the selected beam time a primary beam of fully stripped ^{238}U with an energy of 1 GeV/nucl was impinging on a target combination of 6333 mg/cm² Be and 233 mg/cm² Nb. Together with the FRS standard detector setup and additional aluminium degrader thickness of 4200 mg/cm² the initial settings for all magnets inside the beamline from TA to S4 (see Fig. 1) were calculated with LISE++, and the updated machine model. Furthermore the calculated $B\rho$ values from LISE++ were directly used as input for LSA via the overwrite functionality, allowing operators to circumvent the automatic energy-loss calculations. For the secondary beam fragments the same setup was used with the difference that the FRS was tuned to $^{134}\text{Te}^{52+}$

The calculated currents and rigidities were then compared via

$$\Delta x_{rel} = \frac{x_{calc} - x_{exp}}{x_{exp}} \quad (1)$$

where x denotes either the current or magnetic rigidity and $x_{calc,exp}$ the calculated and experimental values respectively. Assuming that no hysteresis occurs the current should follow the rigidity only via a calibration curve and thus produce redundant results. Nevertheless, the calibration curves of the individual dipoles differ, so that the resulting current varies slightly.

Results

The results focus only on the 4 main dipole magnets of the FRS since these affect the passing of the beam with the highest sensitivity.

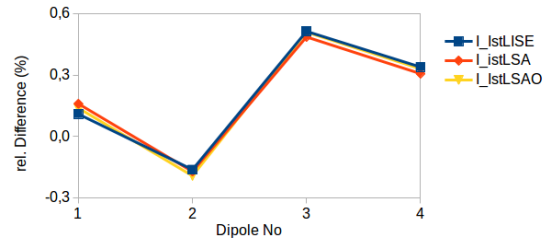


Figure 7: Relative current difference in percent for a primary beam setting (^{238}U at 1 GeV/nucl)

From Fig. 5 one can see that the outgoing energy of the beam depends mostly on the incoming energy and the thickness of the used target material. Since the energy loss calculation is done via ATIMA, the resulting error is given by the accuracy of the thickness of the matter, which for the used devices varies in the order of 1 mg/cm². If one takes this value and continues the calculations for magnetic rigidity, which depends on the beam energy, and subsequently the current, which depends on the rigidity, one finds that the resulting uncertainty is many orders of magnitude smaller than the resulting value for the relative differences and therefore negligible.

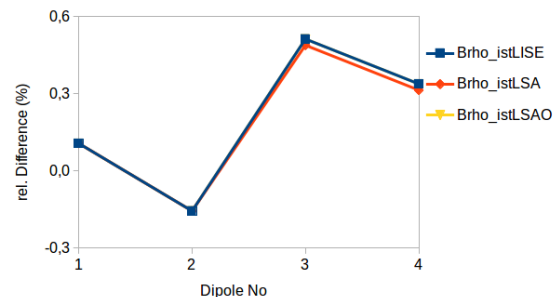


Figure 8: Relative rigidity difference in percent for a primary beam setting (^{238}U at 1 GeV/nucl)

The resulting values can be seen in Fig. 7 to 10 where the results for LISE++ are displayed in blue, the overwrite method in yellow and the updated model in red. One can directly see that in all cases an accuracy in the order of less than 1% can be achieved for all dipoles for both primary as well as secondary beams. It stands out that the current

iteration of the machine model reproduces the experimental settings with an equivalent

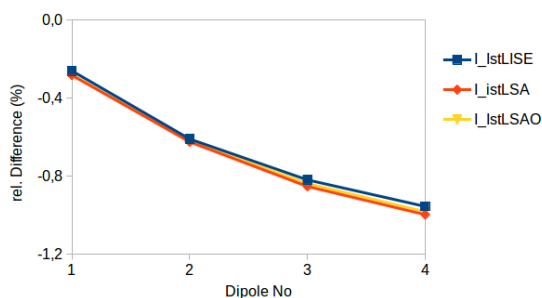


Figure 9: Relative current difference in percent for a secondary beam setting (^{134}Te)

accuracy to LISE++ for all four dipoles. A relative deviation in the order of less than 1% may cause the beam to be off center, the beam could still get lost during transfer from the target area of the FRS to the respective end focal plane. It is important to note that these initial settings should be considered as such and still require manual optimization and tuning by the operator.

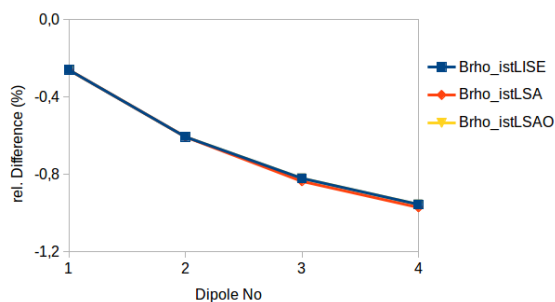


Figure 10: Relative rigidity difference in percent for a primary beam setting (^{134}Te)

CONCLUSION

It was possible to design the machine model of the FRS with all devices from TA to S8 including matter and detectors in the LSA framework, to implement energy-loss calculations and to build new parameter hierarchies for the five different types of matter encountered inside the FRS: detectors, targets, target ladders, degraders and degrader disks. The machine model was tested during engineering runs in April 2019 at the GSI facility at the FRS, which demonstrated that the current machine model and control system may be used to safely operate the FRS and transfer the main beam from TA to S4. Devices and machines, including SIS18, CRYRING and FRS were able to be operated at beamtimes in 2018/2019. A benchmark with former experimental settings showed that the new model is able to reproduce the settings with a relative accuracy in the order of less than 1%, equivalent to LISE++ and energy-loss over-

write by directly inputting rigidity values for the magnet groups which has been used prior to automatic setting of rigidities by LSA. Furthermore updates in ATIMA from Version 1.3 to 1.41 improved the energy-loss calculations at low energies, and new functionalities like hysteresis cycling for dipoles, automatic drive update, target steering, manual overwrite and $B\rho$ selection in slits have been added and proven to work.

REFERENCES

- [1] H. Geissel *et al.*, "The GSI projectile fragment separator (FRS): a versatile magnetic system for relativistic heavy ions," *Nucl. Instr. and Meth. B*, vol. 70, no. 1, pp. 286-297, Aug. 1992.
- [2] A. Prochazka, Justus-Liebig-Universität Gießen, Dissertation: "Nuclear Structure Studies Via Precise Momentum Measurements" (2011).
- [3] H. Geissel *et al.*, Technical Design Report on the Super-FRS (2009), <https://core.ac.uk/download/pdf/52545310.pdf>
- [4] M. Bai *et al.*, "Challenges of FAIR Phase 0", in *Proc. IPAC2018*, Vancouver, BC, Canada, THYGBF3, pp 2947. doi:10.18429/JACoW-IPAC2018-THYGBF3
- [5] H. Geissel *et al.*, "The Super-FRS project at GSI," *Nucl. Instr. and Meth. B*, vol. 204, no. 1, pp. 71-85, May 2002.
- [6] M. Lamont *et al.*, LHC Project Note 368 (2005), <http://cds.cern.ch/record/837651/files/project-note-368.pdf>
- [7] O.B. Tarasov, D. Bazin, "LISE++: Radioactive beam production with in-flight separators," *Nucl. Instr. and Meth. B*, 266 (2008), pp. 4657-4664.
- [8] B. Franczak, simulation programme MIRKO, GSI Darmstadt. Also <http://www-linux.gsi.de/~redelbac/MIRKO/>.
- [9] ROOT Data Analysis Framework, <https://root.cern.ch/>.
- [10] D. Ondreka, J. Fitzek, H. Liebermann, and R. Mueller, "Setting Generation for FAIR", in *Proc. IPAC'12*, New Orleans, LA, USA, THPPR001, pp. 3963-3965.
- [11] D. Ondreka, Die Zukunft der Datenversorgung für GSI und FAIR (2009), https://www-acc.gsi.de/wiki/pub/Applications/LsaPresentationsAndPublications/Zukunft_Datenversorgung_GSI_FAIR_20090924.pdf
- [12] H. Weick *et al.*, "Slowing down of relativistic few-electron heavy ions," *Nucl. Instr. and Meth. B*, vol. 164-165, pp. 168-179, Apr. 2000.
- [13] R. Steinhagen, Dry-Run Procedures & Sequencer Tutorial (2017), GSI Darmstadt, https://fair-wiki.gsi.de/foswiki/pub/FC2WG/HardwareCommissioning/Sequencer/20171207_Sequencer_tutorial.pdf
- [14] J.P. Hucka, Technische Universität Darmstadt Master Thesis: "Implementierung und Test eines Settinggenerators fuer den GSI-Fragmentseparator FRS in der LHC Software Architecture LSA" (2016), unpublished.